

Investigation of Plant–Pathogen Interaction by Laser-Based Photoacoustic Spectroscopy

A. Puiu · G. Giubileo · A. Lai

Received: 13 November 2013 / Accepted: 21 October 2014 / Published online: 31 October 2014
© Springer Science+Business Media New York 2014

Abstract The CO₂ laser-based photoacoustic spectroscopy apparatus, constructed at ENEA Frascati (Italy), was applied to monitor trace amounts of ethylene emitted by plants in a stress condition. More specifically, in the present work, the biotic stress response of tomato mutant plants after inoculation with *Phthorimaea operculella* larvae (*Lepidoptera*: Gelechiidae) was investigated. The principle of the method, the photoacoustic setup, the experimental work, and the results are being reported.

Keywords Biotic stress · Ethylene · Laser photoacoustic spectroscopy · Tomato plants

1 Introduction

Plants are exposed to the attack of many biotic aggressors, mainly pathogens and insects. Thus, early warning in case of any contamination with pathogens which permit immediate remedial actions such as the application of a fungicide or another alternative treatment method would prevent significant economical losses. For this purpose, instruments able to provide fast, cost-effective, and non-invasive screening are required. In this work, we applied laser photoacoustic spectroscopy (LPAS) to monitor the healthy condition of two different tomato plant genotypes.

Plants use different mechanisms to protect themselves. For example, signaling molecules such as ethylene (ET), salicylic acid (SA), and jasmonic acid (JA) are involved

A. Puiu · G. Giubileo (✉) · A. Lai
Diagnostic and Metrology Laboratory, ENEA, Via E. Fermi 45, 00044 Frascati, Italy
e-mail: gianfranco.giubileo@enea.it

in systemic plant resistance [1,2]. In particular, ET has been proposed as a messenger during plant–microbe interactions. ET (biological activity at $1 \mu\text{L}\cdot\text{L}^{-1}$ that corresponds to $6.5 \times 10^{-9} \text{ M}$ at 25°C) [3] is a plant growth regulator, and its molecular simplicity is in contrast with its complex role in the physiology of plants [3–5]. To detect traces (as low as the above mentioned value) of ET requires the availability of a highly sensitive detector. By monitoring emitted ET, one can obtain information about plant–pathogen interactions. Based on the photoacoustic (PA) effect, a CO_2 laser-based setup capable of detecting traces of ET emitted by plants at atmospheric pressure has been developed. The LPAS technique offers an elegant solution to this problem (sensitivity typically under 1 ppbv and high accuracy) for small molecules and, at the same time, possesses a time resolution on the order of a few minutes. Despite being older than 50 years, LPAS proved suitable in a diversity of applications based on real-time non-invasive analysis of gases, especially in the fields of medicine, biology, and environment monitoring, where high stability, selectivity, and sensitivity are impetuses [6–11]. Because the photoacoustic signal generated by the pressure modulation in the PA cell is directly proportional to the power of the excitation source, intense lasers are required to produce a detectable signal due to the very low amount of gas emitted by a single plant.

In the present experiment, the LPAS system that provides continuous information about sub-ppb fluctuations of the ET concentration was applied to monitor the time evolution of ET released by healthy tomato plants as well as by tomato plants infected with the *Phthorimaea operculella* larvae pathogen.

Tomato plants, both wild types and mutants, aging from 60 to 120 days were studied.

2 Experimental Apparatus and Procedures

2.1 LPAS Setup

LPAS measures an effect induced due to the absorption of light rather than the absorption itself. A quantum of radiation at a certain wavelength is absorbed by a given molecule only if the energy of the incoming photon energy matches the energy gap existing between the ground state and an excited state of the molecule. Infrared radiation makes the transitions between vibrational–rotational levels accessible. The $10.532 \mu\text{m}$ infrared radiation emitted by the CO_2 laser (10P(14) line) nearly coincides with one specific roto-vibrational transition of ET. This fact allows us to reach a high detection specificity (Fig. 1). In fact, at this wavelength, the absorption of other constituents in the air is negligible, except for H_2O and CO_2 . However, the latter can be eliminated by using traps (KOH or soda lime scrubber for CO_2 and cryogenic trap for H_2O).

As a consequence of the absorption of radiation by the gaseous sample, acoustical waves are produced by the gas pressure modulation in a cylindrical resonator (photoacoustic PA cell) equipped with sensitive miniaturized microphones. Therefore, the incoming laser beam was modulated at an audio-frequency (550 Hz) by means of a mechanical chopper. Upon undergoing selective excitation, ET molecules can then follow two kinds of de-excitation pathways: radiative decay (fluorescence, phosphorescence) or the non-radiative decay (energy transfer to different species through

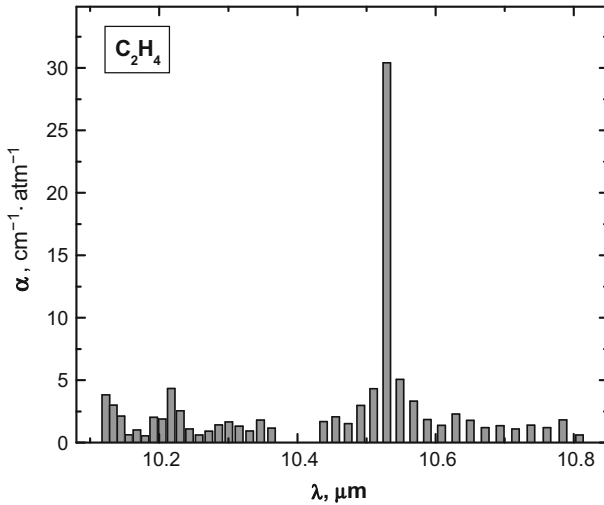


Fig. 1 Absorption coefficients α of ET at different wavelengths of the CO₂ laser. The absorption is maximal ($\alpha = 30.4 \text{ atm}^{-1} \cdot \text{cm}^{-1}$) at 10P(14) laser line

Table 1 Absorption coefficients α ($\text{atm}^{-1} \cdot \text{cm}^{-1}$) for ethylene (ET) at two lines (949.48 cm^{-1} and 944.19 cm^{-1}) of the CO₂ laser used for trace detection of ET [9]

Spectral line	Wavelength (μm)	Frequency (cm^{-1})	$\alpha_{\text{C}_2\text{H}_4}$ ($\text{atm}^{-1} \cdot \text{cm}^{-1}$)
10P(14)	10.53	949.48	30.40
10P(20)	10.59	944.19	1.84

intermolecular collisions). If wall effects are neglected, the non-radiative decay rate is proportional to the gas pressure. At atmospheric pressure, the radiative decay time is typically 10^{-2} s, while the non-radiative decay is much faster (10^{-5} s to 10^{-7} s). This means that the radiative decay can be neglected in comparison with the non-radiative one, and we may consider all the energy as being transferred to the nitrogen molecules (the buffering gas). The periodic energy transfer generates a local periodic thermal modulation in the photoacoustic resonator that, in turn, determines a gas pressure modulation: the cyclic pressure modulation is the photoacoustic (PA) signal. The PA signal is transformed into an electric signal by the microphones. The amplitude of the PA signal is proportional to the number of absorbing molecules. In addition to the PA signal given by the laser wavelength absorbed by ET (the 10P(14) laser line), the PA signal given by a wavelength not absorbed by ET (the 10P(20) laser line) is also taken into account to evaluate the less significant contribution to the PA signal given by other species different from ET (i.e., residual CO₂). Values of the ET absorption coefficients at 10P(14) and 10P(20) laser lines [9] are reported in Table 1.

A schematic drawing of our experimental apparatus is reported in Fig. 2. The radiation source is a frequency stabilized CO₂ laser source (Ultra Lasertech, Model 8822L) emitting 10 W in the continuous wave mode; the laser emission is line tunable over the $9.2 \mu\text{m}$ to $10.8 \mu\text{m}$ spectral range. The laser radiation is amplitude modulated by

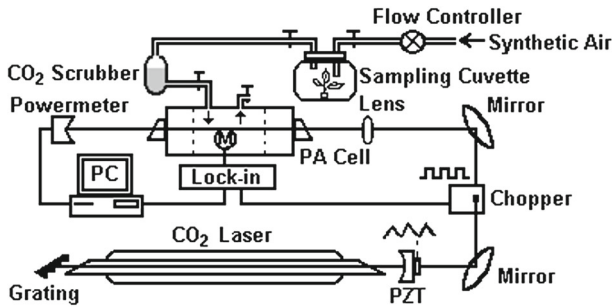


Fig. 2 Schematic view of the experimental setup for LPAS

a mechanical chopper (EG&G, Model 197). The ET detector is a resonant photoacoustic cell (inner volume of 2L, resonant frequency of 550 Hz) equipped with four high sensitivity microphones (Knowles Electronics Inc., USA, Model EK 3033) connected in series, with $40 \text{ mV} \cdot \text{Pa}^{-1}$ total sensitivity. Subsequently, the electric signal from the microphones is amplified by a lock-in amplifier (Stanford Research System, Model SR830 DSP) and directly recorded by a personal computer. The laser beam power is measured by a power meter (LaserProbe, Model Rk-570). All the measurements were conducted under a flowing mixture regime by using synthetic air as the carrier.

This kind of system has already proven adequate for such measurements on gaseous samples from different origins [4–8]. Moreover, other research groups already successfully applied LPAS detection to study plant physiology and plant–pathogen interactions [10–12].

The LPAS setup was calibrated by using a certified bottle of a calibrating mixture (1 ppm C_2H_4 in N_2) provided by Alphagaz. The PA cell was previously evacuated and then filled with 1 atm (1 atm = 1.013 bar) of the calibrating mixture, and the PA signal was accurately recorded. The measurement was repeated at a few different laser power values in order to check the linearity of the photoacoustic effect. The calibrating data have been expressed in $\text{mV} \cdot \text{ppb}^{-1}$, and summarized in Fig. 3. The obtained minimum detectable amount (m.d.a.) of ET was 0.2 ppb.

2.2 Measurement Procedure

The plants were put into a closed glass cuvette shown in Fig. 4, provided with input/output ports to transport air and the ET emitted by the plant into the analyzing cell through small Teflon tubing. The air flux was regulated by high precision flowmeters (Model UR- 4100 by Techno Fittings).

The ET emission expressed in ppb was calculated by using [6]

$$c_{\text{C}_2\text{H}_4} = 0.0953 \left(\frac{V^{14}}{P_L^{14}} - 1.05 \frac{V^{20}}{P_L^{20}} \right) [\text{ppb}], \quad (1)$$

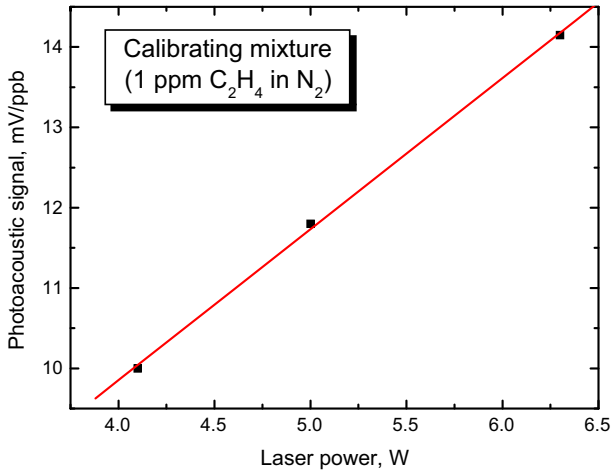


Fig. 3 Calibration of the PA system with the certified gas mixture (1 ppm C_2H_4 in N_2)

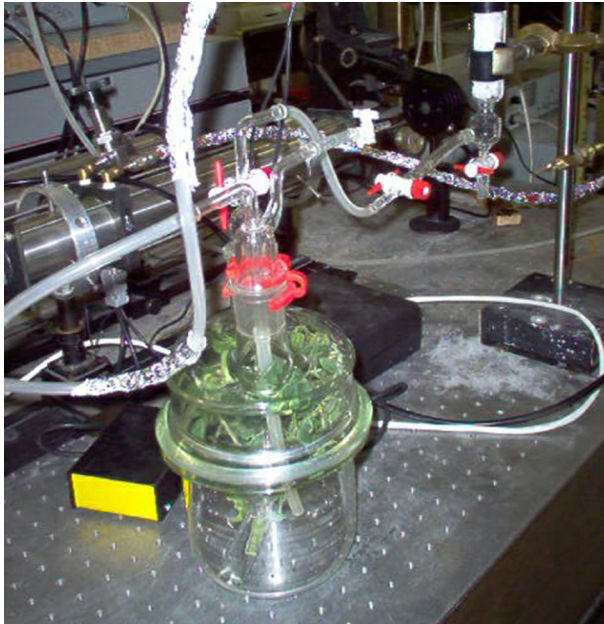


Fig. 4 Sample plant within the measuring cuvette

where V^{14} and V^{20} are the PA signals measured on 10P(14) and 10P(20) laser lines; P_L^{14} and P_L^{20} are the unmodulated laser powers on 10P(14) and 10P(20) lines, respectively. These two laser emissions were chosen as ON/OFF wavelengths for ET. Taking into account the gas flow rate inside the measuring cell ($3 L \cdot h^{-1}$), the final results are expressed in $nL \cdot h^{-1} \cdot g^{-1}$. The rate of the ET released by plants during the measurements in a continuous mode was calculated as

Table 2 Dry weight of each analyzed sample

Sample	DW(g)
<i>rin-c</i>	1.710
<i>rin-i</i>	1.460
v711-231-c	1.820
v711-231-i	0.892

DW dry weight; *rin-c* control *rin* genotype (healthy); *rin-i* inoculated *rin* genotype; v711-231-c control wild type genotype (healthy); v711-231-i inoculated wild type

$$R(t) = c(t) \times \phi / DW, \quad (2)$$

where $R(t)$ is the release rate of ET (in $\text{nL}\cdot\text{h}^{-1}\cdot\text{g}^{-1}$), $c(t)$ is the gas concentration of ET ($\text{nL}\cdot\text{L}^{-1}$) measured by the LPAS system at time t , ϕ is the air flow rate ($\text{L}\cdot\text{h}^{-1}$), and DW is the sample dry weight (g) gathered after warming the sample in an oven set to low heat (38°C) overnight.

The ET concentration was expressed in $\text{nL}\cdot\text{h}^{-1}\cdot\text{g}^{-1}$, by using the dry weight (DW) of the sample plant reported in Table 2. The contribution given by the residual CO_2 entering the PA cell after passing the scrubber was subtracted from the total PA signal. Being an essential volatile released by all biological systems, CO_2 is present in the analyzed sample and, therefore, is important to eliminate it because it absorbs the laser radiation at the same analytical wavelength as ET. The measurement error was estimated as the standard deviation of the signal amplitude oscillations over 50 repeated acquisition points.

2.3 Biological Material

Tomato mutants, such as *Never-ripe (Nr)*, *ripening-inhibitor (rin)*, *non-ripening (nor)*, and *high-pigment (hp)*, differing from the normal ripening process have been studied. These mutants are characterized by their insensitivity to ET, accumulation of lycopene, and moderate pathogen resistance. In the study described here, tomato mutants with a defective ET response and wild type plants were used. Samples grown in a climatic chamber at 25°C were infected with 100 *P. operculella* larvae.

The v711-231 genotype was assumed as the control line (wild type), while *rin* (*ripening-inhibitor*) served as the modified line. The v711-231 isogenic line with anthocyanine is similar to a normal control. The tomato *rin* mutant is a single locus mutation affecting different stages in the synthesis of ET and blocking the normal ripening response to exogenous ET. *Rin* mutant fruit fails to synthesize climacteric ET or accumulate lycopene (red carotenoid), in addition to being deficient in softening and remaining resistant to microbial infection.

3 Results

Emission of ET (within a time interval extending from 30 min to 5 h following the inoculation of pathogen) was recorded in a continuous mode. The resulting ET profiles

for the *rin* plant (both infected plant and healthy plant) are shown in Fig. 5. The same procedure was applied to the control genotype (v711-231); both responses (healthy v711-231 as well as diseased v711-231) are shown on the same graph in Fig. 6. The evolution of ET biosynthesis from each infected plant shows some difference in comparison with non-infected ones. The burst of ET was evident at approximately one and a half hour following the inoculation for the healthy mutant and approximately 2 h for the healthy control; the peak emission values are reported as a bar-graph in Fig. 7. The

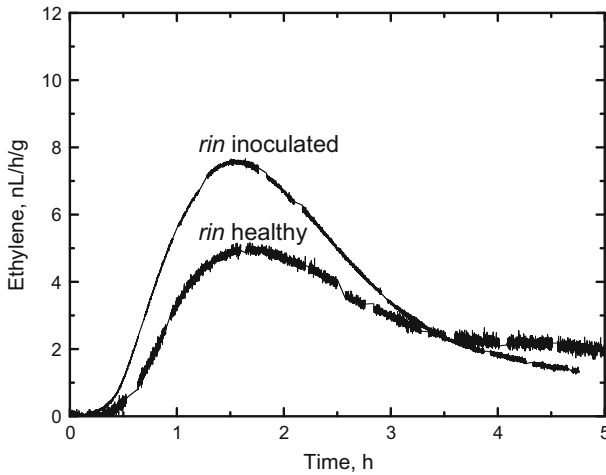


Fig. 5 Comparison of ET emission profiles obtained for healthy *rin* tomato plant and *rin* tomato plant infected with *P. operculella*. The error, estimated as the standard deviation of the signal amplitude oscillations over 50 repeated acquisition points, was 1.7% at the maximum of the curve for healthy *rin* and 0.86% for infested *rin*

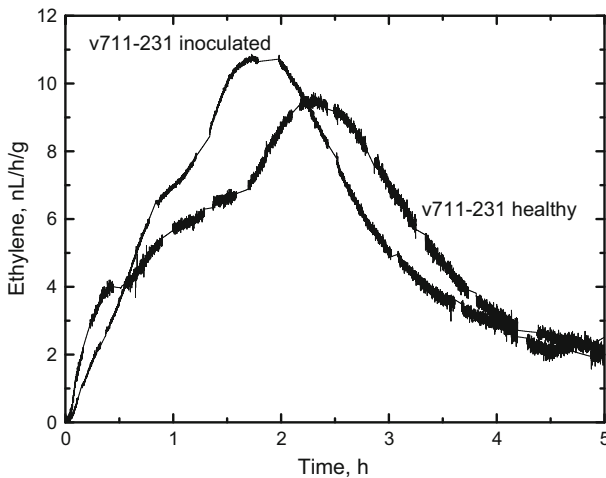


Fig. 6 Emission profile of ET obtained for healthy and *P. operculella* infested v711-231 tomato plants. The error, estimated as the standard deviation of the signal amplitude oscillations over 50 repeated acquisition points, was 0.9% at the maximum of the curve for the healthy plant and 0.3% for the inoculated plant

peak of ET emission in the *rin*-infected sample was higher than in the healthy plant; the same effect was measured for v711-231. Moreover, in the v711-231 genotype the peak emission from the inoculated sample was more rapid than in the healthy one; the curve features a peculiar structure, the origin of which might be related to the plant genotype, since it looks to be quite similar for healthy and inoculated samples. The ET emission measured from the infected plant was higher than in the healthy ones; the LPAS setup was able to point out the differences, as expected.

In order to account for the natural variability of the biological samples, we simulated the ET profiles by adding 15 % of variability to the original measured data. As can be observed from Fig. 8, the principal component analysis (PCA) applied to these data gives simultaneous information about the healthy state of the plants as well as the plant genotype by separating the samples in well-defined groups which allow for their rapid identification.

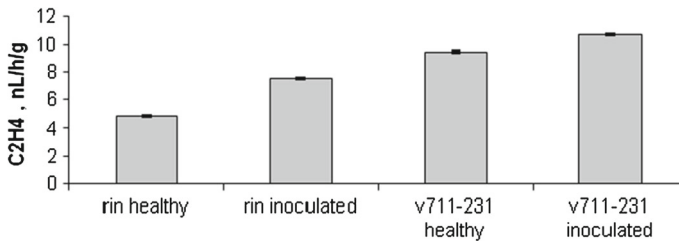


Fig. 7 Peak values of ET biosynthesis in control (v711-231) and mutant (*rin*) tomato plants

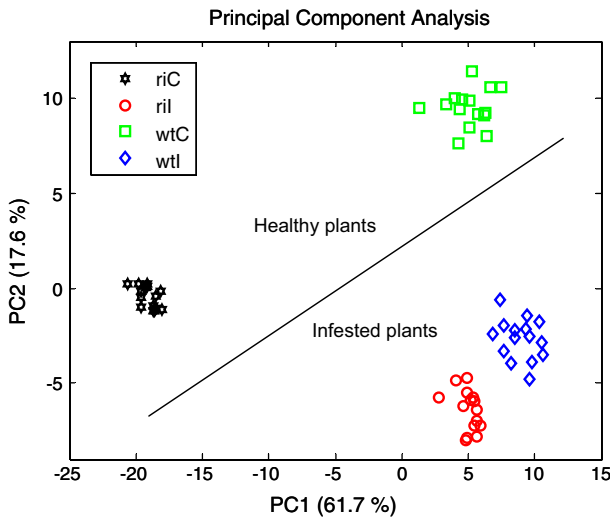


Fig. 8 PCA applied to ET emission profiles (original data and data simulated by considering 15 % of biological variability) for different samples: *rin*-C (*rin* control), *rin*-I (*rin* inoculated), *wt*-C (*wild type* control), and *wt*-I (*wild type* inoculated)

4 Conclusion

The obtained results provide a qualitative indication about the plant response to the stress generated by a pathogen attack. Although some differences between infected and healthy plants have been documented in the experiment here, additional experimental studies on different genotypes and pathogens are required for a better understanding of the plant–pathogen interaction. In any case, the capability of the LPAS setup to detect very low traces of ET in biological samples and to follow their time evolution with high time resolution (minutes) has been confirmed once again. By providing valuable information about the response of the plants to the attack of pathogens, the system could prove useful in plant physiological and agricultural studies. The great advantage of the LPAS-based setup is its intrinsically fast response time that permits real on-line monitoring of very low ET amounts, which is impossible to accomplish by other methods. Furthermore, unlike other analytical techniques, trace gas detection is non-invasive and hence it can be useful in studies on plants, animals, and humans without imposing stress on them. However, its present instrumental complexity still prevents its application in systematic biological investigations, especially in cases where large statistical analysis is required due to the intrinsic variability of the examined samples. The same system can also be used in medicine for breath tests [6, 7]. A similar approach but with another laser source was also applied to detect a variety of industrial gases (including acetylene, carbon monoxide, benzene), nerve gases, explosives (TNT), and poisonous gases (hydrogen cyanide).

Acknowledgment We acknowledge the financial support of the Italian Ministry of Economic Development, in the frame of the National Project MI01_00182 - SAL@CQO.

References

1. A.J. Enyedi, N. Yalpani, P. Silverman, I. Raskin, *Cell* **70**, 879 (1992)
2. L.L.J. Walling, *Plant Growth Reg.* **19**, 195 (2000)
3. F.B. Abeles, P.W. Morgan, M.E. Saltveit Jr., *Ethylene in Plant Biology* (Academy Press, San Diego, 1992)
4. A. Lai, E. Santangelo, D.C. Dumitras, G. Giubileo, V. Fonzo, G.P. Soressi, *Proceedings of the XLVI Annual Congress of Agronomy Genetic* (2002). ISBN 88-900622-3-1
5. A. Lai, L. DeDominicis, R. Fantoni, G. Giubileo, D. Piccinelli, D.C. Dumitras, *Proc. SPIE* **5131**, 295 (2003)
6. G. Giubileo, A. Puiu, G. Argirò, P. Rocchini, E. Borra, *Laser Phys.* **14**, 243 (2004)
7. A. Puiu, G. Giubileo, C. Bangrazi, *Int. J. Environ. Anal. Chem.* **85**, 1001 (2005)
8. G. Giubileo, A. Lai, D. Piccinelli, A. Puiu, *Nucl. Instrum. Methods A* **623**, 778 (2010)
9. R.J. Brewer, C.W. Bruce, J.L. Mater, *Appl. Opt.* **21**, 4092 (1982)
10. S.M. Cristescu, E.J. Woltering, F.J.M. Harren, “Real Time Monitoring of Ethylene During Fungal–Plant Interaction by Laser-Based Photoacoustic Spectroscopy,” in *Food Mycology: A Multifaceted Approach to Fungi and Food*, ed. by J. Dijksterhuis, R.A. Samson (Taylor and Francis/CRC Press, Boca Raton, FL, 2007), p. 27. Print ISBN: 978-0-8493-9818-6, eBook ISBN: 978-1-4200-2098-4, doi:[10.1201/9781420020984](https://doi.org/10.1201/9781420020984)
11. S.M. Cristescu, D. De Martinis, S. te Lintel Hekkert, D.H. Parker, F.J.M. Harren, *Appl. Environ. Microbiol.* **68**, 5342 (2002). doi:[10.1128/AEM.68.11.5342-5350.2002](https://doi.org/10.1128/AEM.68.11.5342-5350.2002)
12. M.W. Sigrist, *Infrared Phys. Technol.* **36**, 585 (1995)